Biochimie 93 (2011) 988–994

Contents lists available at ScienceDirect

Biochimie

journal homepage: www.elsevier.com/locate/biochi

Research paper

Detection of liposome membrane viscosity perturbations with ratiometric molecular rotors

Matthew E. Nipper [a], Marianna Dakanali [b], Emmanuel Theodorakis [b], Mark A. Haidekker [a,*]

[a] University of Georgia, Faculty of Engineering, 597 D.W. Brooks Drive, Athens, GA 30602-4435, USA
[b] University of California, San Diego, Department of Chemistry and Biochemistry, 9500 Gilman Drive, La Jolla, CA 92093-0358, USA

ARTICLE INFO

Article history:
Received 23 October 2010
Accepted 14 February 2011
Available online 24 February 2011

Keywords:
Molecular rotor
Liposome
FRAP
Membrane viscosity
Fluidity

ABSTRACT

Molecular rotors are a form of fluorescent intramolecular charge-transfer complexes that can undergo intramolecular twisting motion upon photoexcitation. Twisted-state formation leads to non-radiative relaxation that competes with fluorescence emission. In bulk solutions, these molecules exhibit a viscosity-dependent quantum yield. On the molecular scale, the fluorescence emission is a function of the local free volume, which in turn is related to the local micro-viscosity. Membrane viscosity, and the inverse; fluidity, are characteristic terms used to describe the ease of movement withing the membrane. Often, changes in membrane viscosity govern intracellular processes and are indicative of a disease state. Molecular rotors have been used to investigate viscosity changes in liposomes and cells, but accuracy is affected by local concentration gradients and sample optical properties. We have developed self-calibrating ratiometric molecular rotors to overcome this challenge and integrated the new molecules into a DLPC liposome model exposed to the membrane-fluidizing agent propanol. We show that the ratiometric emission intensity linearly decreases with the propanol exposure and that the ratiometric intensity is widely independent of the total liposome concentration. Conversely, dye concentration inside liposomes influences the sensitivity of the system. We suggest that the new self-calibrating dyes can be used for real-time viscosity sensing in liposome systems with the advantages of lifetime measurements, but with low-cost steady-state instrumentation.

1. Introduction

Membrane viscosity is a characteristic term that describes the ease of movement within the phospholipid bilayer [1]. Recently, membrane viscosity has been investigated as a possible approach to indicate physiological processes within the cell [2–5]. Membrane protein functionality, carrier-mediated transport and membrane-bound receptors are directly influenced by membrane viscosity [6,7]. Increases in membrane viscosity have been reported with the onset of atherosclerosis [4], malignancy [8], diabetes [9,10], and hypercholesterolemia [11]. Conversely, a decrease in membrane viscosity has been linked with amyloid precursor protein production in patients with Alzheimer's disease [12]. Probing and quantifying changes in membrane viscosity may prove to be an exceptional tool to cell biologists and clinicians alike.

Mechanical methods such as magnetic microbead based rheometry [13] and micropipette aspiration [14] both induce a physical probing force which may impact the physiological state of the membrane. Both micropipette aspiration and magnetic rheometry return averaged values for a large region and cannot reveal local variations. Furthermore, these methods are surface-based and are unable to characterize inner core dynamics of the membrane. For the same reasons, these methods are limited in both temporal and spatial resolution. Fluorescence-based methods have become very popular for measuring membrane viscosity over the past 30 years. The most well-established and documented methods are fluorescence anisotropy and fluorescence recovery after photobleaching (FRAP).

FRAP experiments are considered the "gold standard" technique for monitoring protein mobility and activity within the cell. FRAP experiments are performed by photobleaching a population of fluorophores within a membrane, monitoring the diffusive recovery of intact fluorophores, and computing the rate constants for the recovery. The resulting rate constants are directly proportional to the membrane viscosity. The resulting rate constants have been used to calculate bulk viscosity values for lateral diffusion within the membrane. Viscosity values found by using this method provide an averaged metric for the area of the bleached spot, and the spot size limits the spatial resolution. FRAP has been used to characterize membrane-bound protein mobility [15,16] and the effects of

* Corresponding author. Tel.: +1 706 542 0885.
E-mail address: mhaidekk@uga.edu (M.A. Haidekker).

0300-9084/$ – see front matter © 2011 Elsevier Masson SAS. All rights reserved.
doi:10.1016/j.biochi.2011.02.002

mobility on gene expression [17]. Fluorescence anisotropy has been used, for example, to study DNA-protein interactions [18] along with the membrane viscosity altering effects of lipid peroxidation [19]. Both fluorescence anisotropy and FRAP require unique considerations when designing an experiment. A single FRAP experiment may take several minutes for bleaching and recovery, thus making real-time observations difficult. The accuracy of fluorescence anisotropy experiments is highly dependent on quality and alignment of the polarizers, to name two examples.

With molecular rotors, an alternative to the traditional fluorescence-based methods has emerged in recent years [20]. Molecular rotors are a unique class of fluorophores that exhibit a free volume-dependent quantum yield. This sensitivity results from two competing deexcitation paths, radiative photon release and a non-radiative deexcitation through intramolecular rotation. The rotation rate of these molecules is directly impeded by the local molecular free volume, which is a function of the local micro-viscosity. This behavior allows the inference of viscosity properties by measuring changes in the quantum yield. Quantum yield ϕ_F and viscosity η are related through a power-law [21],

$$\phi_F = \phi_0 \cdot \left(\frac{\eta}{\sigma}\right)^x \quad (1)$$

where ϕ_0 is the intrinsic quantum yield, i.e., the propensity of a specific dye to return to the ground state via the planar radiative pathway, σ reflects the dye's motion in the excited state and the associated electrostatic forces [22], and x depends on the dye and the local microenvironment. The dye constant σ has units of viscosity [22]. Because fluorescence emission is proportional to the quantum yield, simple emission intensity measurements advertise themselves for probing the local micro-viscosity. Previous research efforts have focused on derivatives of (2-carboxy-2-cyanovinyl)-julolidine (CCVJ), which show a single emission that obeys Equation (1). In particular, a farnesyl linked CCVJ derivative, abbreviated FCVJ, has been shown to exhibit local viscosity-dependent quantum yield in liposomes [23]. We have successfully incorporated FCVJ into a liposome model system and evaluated the effects of short and long chain alcohols, cholesterol, and various pharmaceutical compounds on membrane viscosity. Furthermore, FRAP experiments with increasing concentrations of cholesterol were used to compare the viscosity sensing capabilities. FRAP-derived viscosity and molecular rotor-derived intensity correlated highly, although FRAP reports long-range viscosities governed by translational diffusion, whereas molecular rotors provide intensity data governed by local micro-viscosity and rotational diffusion [21], two different metrics that cannot in all cases be directly compared.

Fluorescence intensity is primarily dependent on the local concentration of the fluorophore. Signal dependence on intensity values have led to the introduction of ratiometric sensing schemes to correct for concentration inconsistencies [24,25]. Luby-Phelps et al. [24] used a mixture of hydrophilic Cy3 and Cy5 dyes where size differences may lead to different local accumulation and therefore to different ratios. The styryl-based dye introduced by Wandelt et al. [25] exhibits polarity-sensitivity. We have developed a covalently linked ratiometric rotor that features a reference signal that is statistically viscosity-insensitive and a molecular rotor that is typically insensitive towards the polarity of the environment [26]. The ratiometric molecular rotors used in this study are composed of viscosity-insensitive reference fluorophore conjugated to a traditional molecular rotor [27]. The covalent linkage ensures equal local concentrations for the reference and the rotor, and we expect local concentration effects to be fully accounted for: At low dye concentrations and with negligible inner filter effect, the emission intensity I_{em} depends on a fluorophore's quantum yield ϕ_F according to Equation (2),

$$I_{em} = I_{ex} \cdot G \cdot c \cdot \phi_F \quad (2)$$

where I_{ex} is the intensity of the excitation beam, G is an instrument gain factor, and c is the dye concentration. By measuring the emission of the molecular rotor and dividing it by the emission of the reference fluorophore, the instrument-dependent factors in Equation (2) cancel out, and Equation (1) can be expressed in terms of the ratio of rotor intensity I_{Rotor} to reference intensity I_{Ref},

$$\frac{I_{\text{Rotor}}}{I_{\text{Ref}}} = \frac{\phi_0}{\phi_{\text{Ref}}} \cdot \left(\frac{\eta}{\sigma}\right)^x \quad (3)$$

where ϕ_{Ref} is the quantum yield of the reference fluorophore, which is usually close to unity. In this study, we examined to what extent these theoretical considerations can be applied to liposomes in practical experiments. For this purpose, we used a recently developed molecular rotor with a thiophene backbone [28] and covalently attached a coumarin reference unit. We examined this dye combination in an alcohol viscosity gradient to validate the assumption in Equation (3). Next, we integrated the dye into a liposome model and examined the liposome response to propanol. We finally assessed the concentration sensitivity of the ratiometric sensing system.

2. Materials & methods

2.1. Synthesis of ratiometric molecular rotor *1*

The ratiometric molecular rotor **1** was synthesized following the scheme provided in Fig. 1. The synthesis was achieved in three steps as follows.

Preparation of linker **4**: To a round bottom flask containing a solution of the BOC-protected amino alcohol **3** (5.41 mmol) and cyanoacetic acid (**2**) (3.44 mmol) in 10 ml of anhydrous DCM, EDC (5.43 mmol) and HOBT (5.43 mmol) were added. The formation of the product was monitored by TLC and was completed after overnight stirring at room temperature. The crude mixture was concentrated under reduced pressure and the product was purified via flash chromatography (10–30% EtOAc–hexanes).

Ester **4**: 68% yield; yellow oil; ^{1}H NMR (400 MHz, $CDCl_3$) δ 4.81 (s, 1H), 4.22 (t, 2H, $J = 6.2$ Hz), 3.47 (s, 2H), 3.16 (m, 2H), 1.81 (m, 2H), 1.38 (s, 9H); ^{13}C NMR (100 MHz), $CDCl_3$ δ 163.0, 155.9, 113.0, 79.2, 64.1, 36.8, 28.7, 28.2, 24.6; HRMS calc for $C_{11}H_{18}N_2O_4Na$ $(M + Na)^+$ 265.1159 found 265.1163.

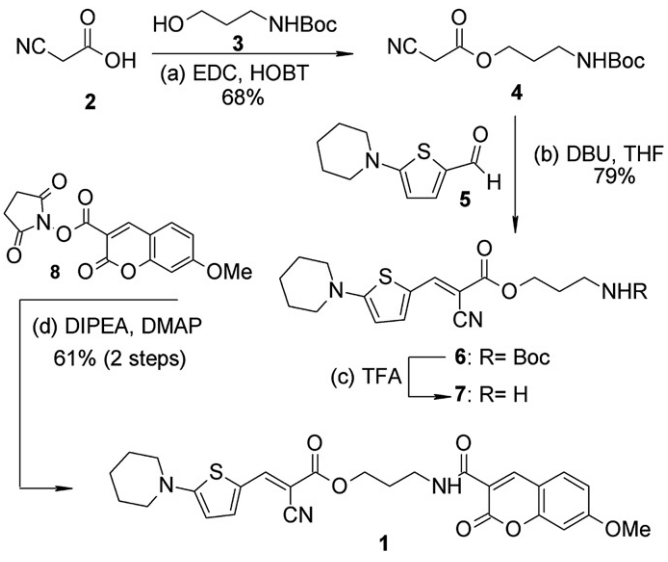

Fig. 1. Synthesis of the ratiometric molecular rotor **1**.

Synthesis of molecule **6**: To a round bottom flask, compounds **4** (1.24 mmol) and **5** (1.24 mmol) were dissolved in dry THF (10 ml). To that, DBU (1.44 mmol) was added and left stirring at room temperature. Upon completion, the crude solution was concentrated under reduced pressure and the product was purified via flash chromatography (10–30% EtOAc–hexanes).

Ester **6**: 79% yield; yellow solid; ^{1}H NMR (400 MHz, $CDCl_3$) δ 8.03 (s, 1H), 7.44 (bs, 1H), 6.11 (d, 1H, $J = 4.6$ Hz), 4.83 (bs, 1H), 4.30 (t, 2H, $J = 6.1$ Hz), 3.45 (m, 4H), 3.23 (m, 2H), 1.90 (m, 2H), 1.71 (m, 6H), 1.44 (s, 9H); ^{13}C NMR (100 MHz, $CDCl_3$) δ 169.5, 165.3, 155.9, 146.4, 144.0, 119.8, 118.4, 104.9, 79.1, 62.7, 51.2, 37.3, 29.2, 28.4, 25.0, 23.5; HRMS calc for $C_{21}H_{29}N_3O_4SNa$ $(M + Na)^+$ 442.1771 found 442.1776.

Synthesis of ratiometric dye **1**. A TFA solution was prepared by combining 5 ml of TFA with 0.1 ml of anisole in 4.9 ml of DCM. 2.76 ml of this solution was added to **6** (0.286 mmol) and the reaction was left stirring at room temperature. After 30 min, reaction was completed and the solution was concentrated, rinsed with toluene (4×10 ml), concentrated, and dried under high vacuum to yield **7**. To a round bottom flask containing **7** dissolved in dry DCM (2 ml); DMAP (0.029 mmol), **8** (0.272 mmol), and DIPEA (0.572 mmol) were added. The reaction was left stirring at room temperature and monitored by TLC. Upon completion, the reaction was concentrated under reduced pressure and purified via flash chromatography (10–20% EtOAc–hexanes).

Dye **1**: 61% yield; orange solid; ^{1}H NMR (400 MHz, $CDCl_3$) δ 8.90 (bs, 1H), 8.82 (s, 1H), 8.03 (s, 1H), 7.57 (d, 1H, $J = 8.7$ Hz), 7.43 (s, 1H), 6.92 (dd, 1H, $J = 2.3$ Hz, $J = 8.7$ Hz), 6.84 (d, 1H, $J = 2.3$ Hz), 6.09 (d, 1H, $J = 4.6$ Hz), 4.33 (t, 2H, $J = 6.2$ Hz), 3.90 (s, 3H), 3.58 (m, 2H), 3.43 (m, 4H), 2.05 (m, 2H), 1.69 (m, 6H); ^{13}C NMR (100 MHz, $CDCl_3$) δ 169.4, 165.1, 164.7, 162.3, 161.7, 156.6, 148.3, 146.4, 130.9, 119.8, 118.3, 114.7, 113.9, 112.4, 104.8, 100.3, 62.9, 56.0, 51.2, 36.8, 28.8, 25.0, 23.5; HRMS calc for $C_{27}H_{27}N_3O_6SNa$ $(M + Na)^+$ 544.1513 found 544.1517.

2.2. Viscosity gradient

The viscosity sensitivity of the ratiometric dye was established in gradient experiments with fluoroscopy-grade methanol, ethylene glycol and glycerol (Sigma–Aldrich). Excitation scans were first performed on the lowest viscosity sample in the fluorospectrophotometer (Fluoromax-3, Jobin-Yvon, Edison, NJ). The optimal excitation wavelength was then used throughout the gradient experiment. This step is performed to provide a uniform standard for the fluorophore's sensitivity to changes in bulk viscosity. This also serves the dual purpose of observing the non-viscosity-sensitive reference and the molecular rotor spectra. With reference to Equation (3), a plot of the intensity ratio over viscosity in a double-logarithmic plot should follow a straight line with slope x and an intercept for $\eta = 1$ at $\phi_0/\phi_{\mathrm{Ref}}\sigma^x$.

2.3. Liposome electroformation

All agents and alcohols were purchased from Sigma–Aldrich unless otherwise stated. The ratiometric molecular rotors were synthesized by our own group [29]. A 10 mM stock solution of each rotor was prepared in chloroform. 4 μL of each stock was added to 200 μL of 1,2-D-lauroyl-sn-glycero-3-phosphocholine (DLPC:chloroform Avanti Polar Lipids) in a glass vial. An established electroformation process was performed on platinum electrodes to create giant unilamellar liposomes [30,31]. Prior to formation, the electrode chamber was sonicated and cleaned in Alconox detergent and ethanol respectively for 15 min. A glass syringe, cleaned with chloroform, was used to deposit the rotor/DLPC mixture onto the platinum electrodes. The chamber was placed under vacuum for 30 min to remove any remaining organic solvents. Glass coverslips were placed over the top of the chambers to prevent outside impurities from entering. The chambers were then flooded with 10 ml of a 250 mM sucrose:double distilled water solution. The electroformation process was started by applying a 1 V_{pp}, 10 Hz sinusoidal signal to the two electrodes for 10 min. The frequency was then lowered to 1 Hz for 5 min. The contents of the chambers were then extracted using a sterile syringe (Beckton–Dickinson), and the electrodes were gently rinsed with the suspension solution to remove any remaining liposomes. The final liposome/sucrose suspension was then stored in a clean tube at 10 °C for no more than 24 h.

2.4. Liposome extrusion

400 μL of DLPC:chlorofom (Avanti Polar Lipids) was mixed with 4 μL of 2.5 mM ratiometric dye **1** in dimethyl sulfoxide in a 6 ml glass vial. The solution was evaporated in the presence of N_2 gas, puffed into the opening of the vial. The vial was slowly mixed and rotated by hand to create a film on the surface of the glass vial during evaporation. To rehydrate, 1 ml of 250 mM aqueous sucrose solution was added. The vial was slowly mixed and rotated to create a thin film on the surface of the vial during evaporation. The rehydration stage consisted of adding 1 ml of 250 mM aqueous sucrose solution. The solution was then treated with 3 freeze–thaw cycles consisting of 10 min in 30 °C prior to extrusion. The solution was then lightly mixed during the freeze–thaw cycles to create an opaque slurry. Liposome extrusion was done with a heat block, 1 ml syringe mini-extruder (Avanti Polar Lipids). The rehydrated solution was passed eleven times through a 0.1 μm filter (Avanti Polar Lipids) while the heat block was set at 31 °C. After filtration the solution was diluted to a final volume of 20 ml in 250 mM aqueous sucrose and stored in a glass vial. All liposome preparations were fully measured within 24 h and stored at 4 °C if not used immediately.

2.5. Short chain alcohol sensitivity and gradient

A volume of 500 μL of the electroformation liposome/rotor suspension was added to 500 μL of either 250 mM sucrose (control) or a 250 mM Sucrose solution with 2, 4, 6, 8, and 10% propanol. Propanol was chosen to provide high interfacial energy [32] at low concentrations. $N = 4$ repeated experiments were conducted for each group to ensure statistical robustness. The solution was then gently inverted 5 times and placed into a temperature controlled turret (Quantum Northwest, Liberty Lake, WA), set at 20 °C (well above the transition temperature of −1.8 °C), and equilibrated for 5 min. The sample was then excited at 352 nm in the spectrophotometer (Fluoromax-3) and spectra were gathered for a range of 370–520 nm with slit settings of 5 nm. The peak intensities from all graphs were normalized to their respective means and graphed.

2.6. Rotor and phospholipid concentration effects

Increasing concentrations of ratiometric dye **1** were used in corresponding constant concentrations of phospholipid for the liposome formation step. Once formation was complete, the groups were subdivided into 4 samples and exposed to either a control or 5% Propanol solution following the protocol for the short chain alcohol step. Increasing concentrations of DLPC (Avanti) were paired with a concentration gradient of ratiometric dye **1** following the formation protocol. Correspondingly, the groups were subdivided into 4 samples and exposed to either a control treatment of 250 mM Sucrose or 5% Propanol solution. Fluorescence spectroscopy and ratiometric measurements were used to quantify the effects on rotor emission and subsequent ratiometric calculations.

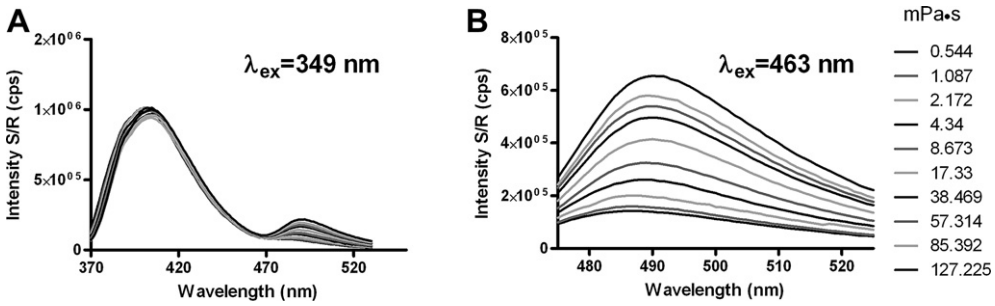

Fig. 2. Indirect excitation of the rotor through reference excitation (A) and direct rotor excitation (B) emission scans of ratiometric dye **1** in ethylene glycol and glycerol gradient. In the reference excitation graph, the low variability of the reference relative to the rotor emission (≈410 nm) highlights the ratiometric properties. The rotor excitation graph confirms the viscosity sensitivity of the molecular rotor.

2.7. Data analysis

Data analysis was performed on the spectra for all sets. The ratiometric data were calculated by dividing the peak intensity of the rotor at 479 nm and reference peak at 410 nm. Equation (4) was used to find the ratiometric intensity I_R for each sample set.

$$I_R = \frac{I_{479}}{I_{410}} \tag{4}$$

To compare the peak intensities, the sets were normalized by the mean intensity. The groups were then compared via the Students *t*-test to confirm a statistically significant difference. The bar graphs show the normalized mean value of $N = 4$ repeated experiments, and all error bars represent the standard deviation. All data analysis was performed with Graphpad PRISM version 4.01.

3. Results & discussion

3.1. Synthesis of ratiometric dye *1*

The synthesis of the ratiometric dye **1** is highlighted in Fig. 1. Esterification reaction between the cyanoacetic acid (**2**) and the Boc-protected amino alcohol **3** yielded the linker **4**. Compound **5** was synthesized according to the literature [28]. Knoevenagel condensation of **5** with the β-cyanoester **4** gave compound **6** in very good yield. Deprotection of the primary amine **6**, followed by coupling with the activated coumarin **8**, yielded the final ratiometric dye **1**. Fluorescence spectra, including the expected viscosity sensitivity of the rotor emission and robustness of the reference against solvent changes were established in the next step.

3.2. Viscosity gradient experiments

The first experiment set was a bulk solvent viscosity gradient in mixtures of ethylene glycol and glycerol. The purpose of this set is to analyze the balance between the reference fluorophore and the molecular rotor portion. It is important to confirm for the ratiometric dyes that the reference dye is indeed viscosity-insensitive and conversely evaluate the rotor sensitivity. These spectral scans reveal information about the dye structure and the effects of manipulating the length of the linker chain between the two fluorophores. In Fig. 2, the spectral scan of ratiometric dye **1** clearly shows two distinct emission peaks, one from the reference unit, and one from the molecular rotor. An increase of the rotor emission can be seen over a wide range of viscosities from pure methanol ($\eta = 0.54$ mPa s) to a 1:1 mixture of ethylene glycol and glycerol ($\eta = 127$ mPa s). Fig. 2A indicates that resonance energy transfer (RET) takes place from the reference to the rotor, allowing simultaneous acquisition of the emission intensities I_{479} and I_{410} (Equation (4)) with a single excitation wavelength. Further calculations yielded a Förster distance R_0 of 19.7 Å and a resulting energy transfer efficiency E of 92% in Equation (5).

$$E = \frac{R_0^6}{r^6 + R_0^6} \tag{5}$$

Coumarins have a very high quantum yield near unity, whereas molecular rotors have typical quantum yields two to three orders of magnitude lower, depending on the viscosity of the environment. The unusually high transfer efficiency has two effects. First, the emission peaks are balanced, and the coumarin peak does not overwhelm the rotor peak. Second, in the region where the dipole–dipole distance r is much smaller than the Förster distance, the first derivative of the transfer efficiency E towards either r or R_0 is very small. Consequently, solvent effects, such as changes of the refractive index, have very little effect on E and make the RET pair robust against the environment.

To confirm the rotors sensitivity to viscosity, the log-transformed peak intensity for both the reference and the rotor were plotted as a function of the log-transformed viscosity in Fig. 3. The purpose of this experiment is to confirm rotor sensitivity and to evaluate

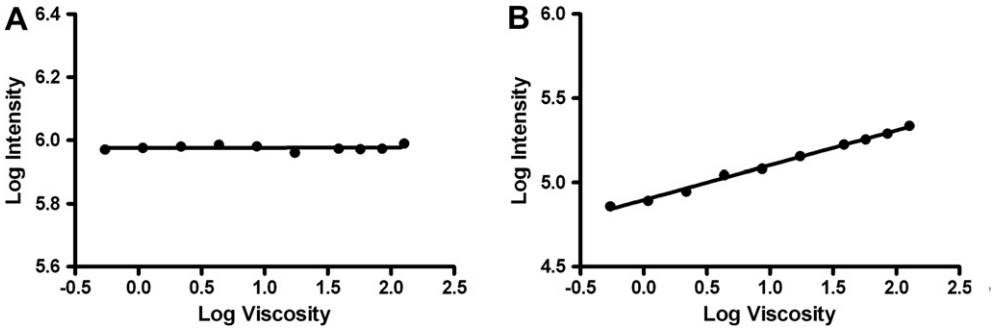

Fig. 3. Plot of ratiometric dye **1** peak emission from the single excitation measurement in Fig. 2. As expected, Fig. 3A exhibits no correlation between viscosity and the reference peak emission. Fig. 3B highlights the molecular rotor emission peak as a function of viscosity and confirms a significant correlation ($R^2 = 0.9945$) with a slope of 0.21.

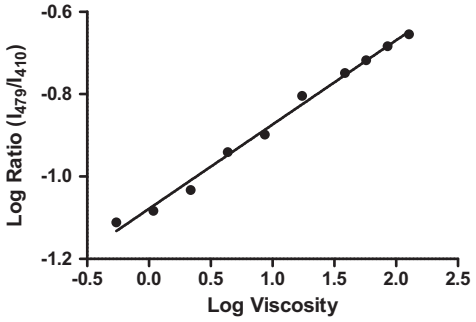

Fig. 4. Calculated emission intensity ratio versus viscosity for ratiometric dye **1**. Ratio I_{479}/I_{410} refers to the peak rotor emission divided by the reference emission for ratiometric dye **1** in ethylene glycol and glycerol. Both the viscosity and ratiometric intensity were log-transformed and then plotted. These values were taken from the reference excitation spectra in Fig. 2.

reference stability. This experiment confirms that the molecular rotor portion of ratiometric dye **1** is indeed sensitive to changes in viscosity and that the reference peak is constant and shows no statistically significant response to the change in solvents and the associated change in viscosity. The secondary molecular rotor peak intensity exhibits a statistically significant ($R^2 = 0.9954$, $P < 0.0001$) power–law relationship with viscosity. The log-transformed data showed a slope of 0.21. The slope for the direct excitation ($\lambda_{ex} = 463$) of the molecular rotor in Fig. 2 as a function of viscosity was 0.28. The slope, which can be interpreted as the sensitivity towards viscosity changes, was markedly lower than the slope of the unconjugated molecular rotor [28]. The decreased sensitivity can be explained by the presence of a hydrophobic element, i.e., the linker. A similar loss of sensitivity was found when the rotor was covalently linked to a hydrophobic surface with a similar linker [33].

By dividing the rotor peak by the reference peak, a unitless ratio I_R is obtained (Equation (4)) that should be robust against variations in concentration. Fig. 4 shows the ratiometric intensity I_R for ratiometric dye **1** as a function of viscosity in a double-logarithmic plot. The significant linear trend in Fig. 4 confirms the response of the ratiometric viscosity sensor to changes in viscosity as predicted in Equation (3) over more than two orders of magnitude.

3.3. Sensitivity in liposomes

The ratiometric, viscosity-sensitive dye, **1**, was used in different concentrations of propanol at 1%, 2%, 3%, 4%, and 5% in aqueous sucrose solution. Examination under an epifluorescent microscope (data not shown) confirmed successful incorporation of the dye into liposomes in both different liposome formation protocols. Exposure to propanol was chosen for these experiments because of the increased ability to intercalate within the membrane compared to shorter chain alcohols [32]. The intercalation of propanol within the membrane results in a relaxation of the compressive modulus resulting in a local free volume increase. The change in free volume is proportional to the decrease in apparent membrane viscosity. A linear trend, similar to the one seen in Fig. 5, was observed with a non-ratiometric molecular rotor and with FRAP in an earlier study [23]. Interestingly, the extruded liposomes exhibited a higher apparent viscosity change as evidenced by the regression slope of the intensity change over the propanol concentration (0.034) compared to the slope of the electroformation group (0.012). This is reasonable considering the average size of extruded liposomes are on the order of 100 nm whereas the electroformation derived liposomes are on the order of several μm. The smaller size of the extruded liposomes results in a higher effective interaction area for the rotor, resulting in a higher sensitivity. Membrane curvature may also play a role in governing the baseline membrane viscosity. As the area per head group is decreased, the free volume is similarly decreased. Future experiments will be required to test this hypothesis. The significant trend demonstrates the ability of the ratiometric technique to report changes in the local viscosity of the phospholipid membrane. However, the relative intensity change reported by the ratiometric system is about one order of magnitude lower than the one reported with the non-ratiometric FCVJ [23]. Given the hydrophobic nature of this compound, we hypothesize that the rotor migrates towards the hydrophobic tail region of the phospholipid in the membrane, where the effects of the alcohol are less pronounced than near the polar head groups. Localization near the center of the bilayer may help explain why a lower exponent (lower apparent sensitivity) was observed than typically seen with molecular rotors in solution where $x \approx 0.6$.

Previous research has reported the membrane viscosity of DPPC liposomes in the range of 127 mPa s [34]. By using Fig. 4 as a calibration curve, we solved Equation (3) for η and found $\eta = 61$ mPa s for DLPC in the absence of propanol. The calculated value is quite reasonable considering the shorter DLPC chains would result in an increased free volume compared to the DPPC. Correspondingly, the increase in free volume would result in a lower membrane viscosity, which is supported with these findings. Continuing this calculation for the entire set of propanol concentrations, the highest concentration of propanol, 5%, reduces the viscosity to 18 mPa s. The ability to measure changes in viscosity using steady-state fluorescence measurements is limited by the ability to accurately measure changes in quantum yield. Because of the two competing pathways between radiative relaxation and rotation, the intrinsic quantum

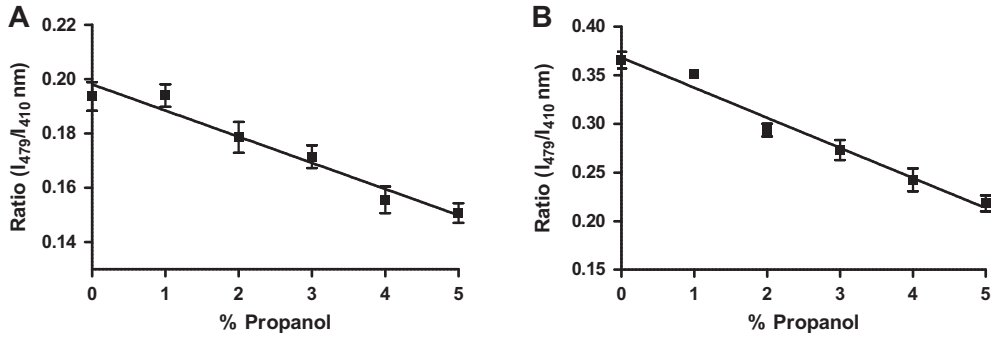

Fig. 5. Ratio of the peak rotor emission to the reference emission for Compound **1** in liposomes formed with both the electroformation (A) and extrusion (B) protocols. The liposomes formed with compound **1** were exposed to increasing concentrations of propanol. Propanol was chosen to achieve the maximum interfacial energy without destroying the membrane. The statistically significant linear response of the ratio for the electroformation ($R^2 = 0.835$) and the extruded ($R^2 = 0.96$) liposomes is indicative to a sensitivity to viscosity changes.

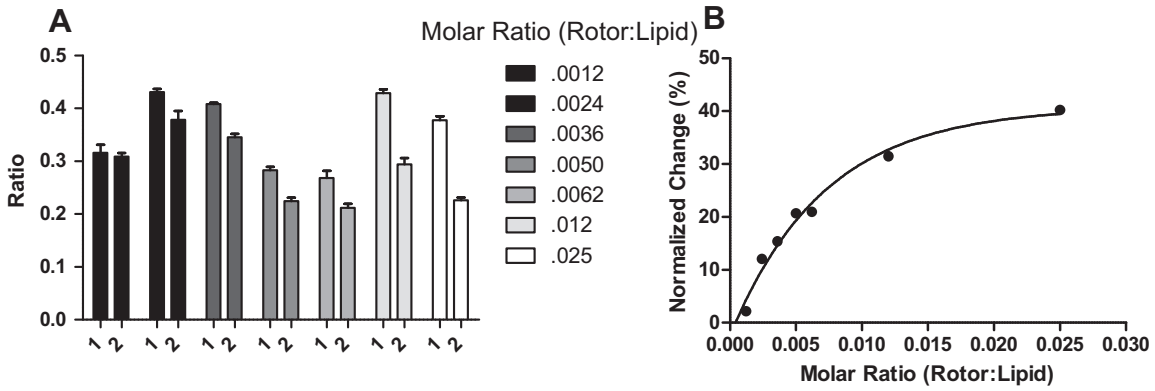

Fig. 6. In Graph A, a series of liposomes with increasing molar ratios of compound **1** to DLPC are exposed to eiter a 250 mM sucrose (control) or a solution of 5% Propanol in 250 mM sucrose. Graph A shows the calculated ratio for the control and 5% Propanol treatments denoted by 1 and 2 respectively. As the molar ratio of compound **1** to DLPC is increasing in each set, the sensitivity to the 5% Propanol treatment is increasing. Graph B plots the normalized ratio change for each of the groups in A as a function of the molar ratio of compound **1** to the lipid used in liposome formation. The sensitivity increases as a function of the molar ratio, then plateaus in an exponential fashion.

yield is often low even in highly viscous solutions. Given these limitations, and assuming the approximate exponent of $x = 0.3$ and an accurate quantum yield measurement to 2 significant figures, Equation (3) is able to relate a 1% change in the local viscosity to 0.3% change in ratiometric intensity. The quantum yield is directly proportional to the emission intensity area under the curve.

3.4. Sensitivity to phospholipid and fluorophore concentration

One of the key claims that result from Equation (3) is the robustness of the ratiometric intensity against fluorophore concentration changes. Fluorophore concentration can be altered in two ways: by altering the fluorophore component in the liposome formation process, and by altering the amount of liposomes in the suspension. In the second case, the total amount of phospholipid influences the turbidity of the sample and may impede fluorescence intensity based measurements. Fig. 6 highlights the effects of increasing fluorophore concentration in the liposomes. The leftmost graph shows a variation in the baseline ratio as the concentration increases. This is most likely due to (1) the non-precise nature of the electroformation process and (2) the influence of higher dye concentrations on the membrane properties. At low concentrations, the low overall emission intensity leads to a poor signal-to-background ratio, reducing sensitivity.

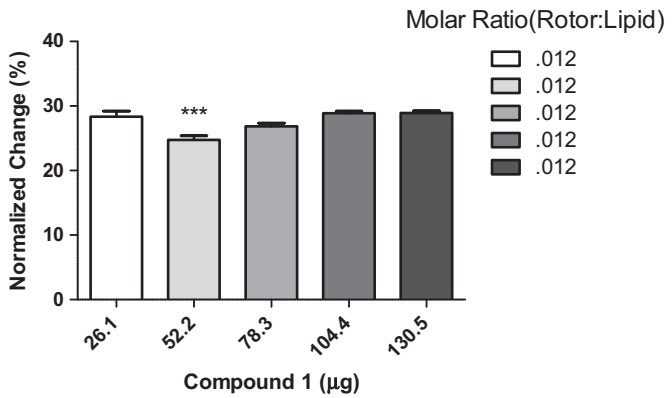

Fig. 7. In this experiment, the concentrations of both compound **1** and DLPC are increased linearly with respect to each other. This results in a constant rotor to lipid ratio as in direct contrast to Fig. 6. The normalized intensity change in the propanol-treated group are shown for increasing concentrations of Compound **1** and DLPC respectively. The results of the ANOVA-test show that only the 10 μL set exhibited a statistically different mean compared to the rest of the group.

At higher dye concentrations, the increased proportion of rotor to phospholipid would increase the surface area for detection resulting in a higher sensitivity. Clearly the apparent sensitivity increases with increasing dye concentration, but the sensitivity gain at higher concentrations is less (Fig. 6B). We found that the sensitivity as a function of concentration can be described well by Equation (6),

$$\Delta I_R = A\left(1 - e^{c/c_0}\right) \tag{6}$$

with the empirical constants A and c_0. This model was chosen because it apparently represented the data well, but there is no theoretical support for this model.

Fig. 7 shows the normalized intensity change in the propanol-treated group for each amount of phospholipid suspension in sucrose solution. This experiment demonstrates that the intensity ratio eliminates some fluid optical properties. In this case, overall liposome concentration (and with it, dye concentration in the suspension) was increased over a factor of five. The change of intensity caused by the application of propanol, however was widely constant. In fact, only the group with 10 μL shows a significant difference from the other groups. Since there is no discernible trend, this deviation may have been caused by experimental error.

4. Conclusions

We have demonstrated the viscosity-sensitive characterization of a ratiometric dye and incorporated the fluorophore into a liposome biomembrane system. Furthermore, we have shown the sensitivity of the molecular rotor once incorporated and tested the robustness of ratiometric sensing techniques. Through calibration with alcohol gradients, ratiometric rotors are capable of reporting membrane viscosity values consistent with those found in literature. The ability to compensate for fluctuations in dye concentration has also been demonstrated. This property makes ratiometric dye systems attractive as an alternative to lifetime measurements: The lifetime τ of a fluorophore is directly linked to its quantum yield ϕ_F and the natural lifetime τ_N through $\phi_F = \tau/\tau_N$, which in turn links lifetime to viscosity through Equation (1), and no instrument-dependent factors (Equation (2)) play a role. Recent studies demonstrate the usability of lifetime measurements with molecular rotors [35–37]. However, molecular rotor lifetimes are in the picosecond range, and expensive lifetime equipment is necessary. Furthermore, molecular rotors tend to exhibit multiexponential decay behavior in low-viscosity environments, which are difficult to interpret. We propose ratiometric dye systems as a low-cost

alternative that relies on steady-state instrumentation, such as conventional epifluorescent microscopes. The ratiometric behavior allows to cancel out instrument-dependent factors (Equation (3)) and provides a direct link between ratiometric intensity and viscosity similar to the link between lifetime and viscosity.

Molecular rotors have an almost instantaneous response to changes in the local viscosity along with a high spatial resolution [20]. The spatial resolution provided by ratiometric molecular rotors may provide the ability to identify and quantify local anisotropic conditions present in the membrane. However, for this purpose, the molecules need to be further modified to force highly specific localization within the bilayer. Molecular reporters have previously been used to monitor conformational changes in proteins [38], polymerization dynamics [39], and membrane viscosity [23,40]. The immediate challenge for molecular rotors is to move from the liposome model into cell culture. In living cells, local concentration gradients play a significant role, and projection microscopy creates a separate artifact where excitation and emission light paths are near-parallel with the cell wall. We expect that the ratiometric measurement methods presented in this study help overcome these artifacts.

Acknowledgements

The authors gratefully acknowledge partial research support from the National Science Foundation through grant CMMI-0652476 and support from the National Institutes of Health through NIH grant 1R21 RR 025358.

References

[1] P. Yeagle, P.L. Yeagle, The Membranes of Cells. Academic Press, San Diego, CA, 1993.
[2] M.O. Eze, Membrane fluidity, reactive oxygen species, and cell-mediated immunity: implications in nutrition and disease, Medical Hypotheses 37 (4) (1992) 220–224.
[3] D.S. Heron, M. Shinitzky, M. Hershkowitz, D. Samuel, Lipid fluidity markedly modulates the binding of serotonin to mouse brain membranes, Proceedings of the National Academy of Sciences of the United States of America 77 (12) (1980) 7463–7467.
[4] T. Koike, G. Ishida, M. Taniguchi, K. Higaki, Y. Ayaki, M. Saito, Y. Sakakihara, M. Iwamori, K. Ohno, Decreased membrane fluidity and unsaturated fatty acids in niemann-pick disease type c fibroblasts, Biochimica et Biophysica Acta (BBA)-Molecular Basis of Disease 1406 (3) (1998) 327–335.
[5] D. Zakim, J. Kavecansky, S. Scarlata, Are membrane enzymes regulated by the viscosity of the membrane environment, Biochemistry 31 (46) (1992) 11589–11594.
[6] K. Shiraishi, S. Matsuzaki, H. Ishida, H. Nakazawa, A. Takada, Impaired erythrocyte deformability and membrane fluidity in alcoholic liver disease: participation in disturbed hepatic microcirculation, Alcohol and Alcoholism 1A (1993) 59–64.
[7] S.J. Singer, G.L. Nicolson, The fluid mosaic model of the structure of cell membranes, Science 175 (23) (1972) 720–731.
[8] M. Shinitzky, Physiology of Membrane Fluidity. CRC, 1984.
[9] O. Nadiv, M. Shinitzky, H. Manu, D. Hecht, C.T. Roberts Jr., D. LeRoith, Y. Zick, Elevated protein tyrosine phosphatase activity and increased membrane viscosity are associated with impaired activation of the insulin receptor kinase in old rats, Biochemical Journal 298 (1994) 443–450.
[10] W. Osterode, C. Holler, F. Ulberth, Nutritional antioxidants, red cell membrane fluidity and blood viscosity in type 1 (insulin dependent) diabetes mellitus, Diabetic Medicine 13 (12) (1996) 1044–1050.
[11] M.M. Gleason, M.S. Medow, T.N. Tulenko, Excess membrane cholesterol alters calcium movements, cytosolic calcium levels, and membrane fluidity in arterial smooth muscle cells, Circulation Research 69 (1) (1991) 216–227.
[12] G.S. Zubenko, U. Kopp, T. Seto, L.L. Firestone, Platelet membrane fluidity individuals at risk for Alzheimer's disease: a comparison of results from fluorescence spectroscopy and electron spin resonance spectroscopy, Psychopharmacology 145 (2) (1999) 175–180.
[13] R. Dimova, B. Pouligny, Optical dynamometry to study phase transitions in lipid membranes, Methods in Molecular Biology 400 (2007) 227–236.
[14] G.B. Nash, W.B. Gratzer, Structural determinants of the rigidity of the red cell membrane, Biorheology 30 (1993) 397–407.
[15] M.B. Elowitz, M.G. Surette, P.E. Wolf, J.B. Stock, S. Leibler, Protein mobility in the cytoplasm of *Escherichia coli*, Journal of Bacteriology 181 (1) (1999) 197–203.
[16] E.A.J. Reits, J.J. Neefjes, From fixed to frap: measuring protein mobility and activity in living cells, Nature Cell Biology 3 (6) (2001) E145–E147.
[17] T. Misteli, Protein dynamics: implications for nuclear architecture and gene expression, Science 291 (5505) (2001) 843–847.
[18] T. Heyduk, Y. Ma, H. Tang, R.H. Ebright, Fluorescence anisotropy: rapid, quantitative assay for protein–DNA and protein–protein interaction, Methods in Enzymology 274 (1996) 492–503.
[19] C. Richter, Biophysical consequences of lipid peroxidation in membranes, Chemistry and Physics of Lipids 44 (2–4) (1987) 175–189.
[20] M.A. Haidekker, E.A. Theodorakis, Molecular rotors – fluorescent biosensors for viscosity and flow, Organic & Biomolecular Chemistry 5 (11) (2007) 1669–1678.
[21] M.A. Haidekker, E.A. Theodorakis, Environment-sensitive behavior of fluorescent molecular rotors, Journal of Biological Engineering 4 (1) (2010) 11–24.
[22] T. Förster, G. Hoffmann, Die viskositätsabhängigkeit der fluoreszenzquantenausbeuten einiger farbstoffsysteme, Zeitschrift für Physikalische Chemie (München). 75 (1971) 63–76.
[23] M.E. Nipper, S. Majd, M. Mayer, J.C.M. Lee, E.A. Theodorakis, M.A. Haidekker, Characterization of changes in the viscosity of lipid membranes with the molecular rotor fcvj, Biochimica et Biophysica Acta (BBA)-Biomembranes 1778 (4) (2008) 1148–1153.
[24] K. Luby-Phelps, S. Mujumdar, R.B. Mujumdar, L.A. Ernst, W. Galbraith, A.S. Waggoner, A novel fluorescence ratiometric method confirms the low solvent viscosity of the cytoplasm, Biophysical Journal 65 (1) (1993) 236–242.
[25] B. Wandelt, A. Mielniczak, P. Turkewitsch, G.D. Darling, B.R. Stranix, Substituted 4-[4-(dimethylamino)styryl]pyridinium salt as a fluorescent probe for cell microviscosity, Biosensors and Bioelectronics 18 (4) (2003) 465–471.
[26] M.A. Haidekker, T.P. Brady, D. Lichlyter, E.A. Theodorakis, Effects of solvent polarity and solvent viscosity on the fluorescent properties of molecular rotors and related probes, Bioorganic Chemistry 33 (6) (2005) 415–425.
[27] M.A. Haidekker, T.P. Brady, D. Lichlyter, E.A. Theodorakis, A ratiometric fluorescent viscosity sensor, Journal of the American Chemical Society 128 (2) (2006) 398–399.
[28] J. Sutharsan, D. Lichlyter, N.E. Wright, M. Dakanali, M.A. Haidekker, E.A. Theodorakis, Molecular rotors: synthesis and evaluation as viscosity sensors, Tetrahedron 66 (14) (2010) 2582–2588.
[29] D. Fischer, E.A. Theodorakis, M.A. Haidekker, Synthesis and use of an in-solution ratiometric fluorescent viscosity sensor, Nature Protocols 2 (1) (2007) 227–236.
[30] M. Angelova, S. Soleau, P. Meleard, F. Faucon, P. Bothorel, Preparation of giant vesicles by external AC electric fields. Kinetics and applications, Trends in Colloid and Interface Science VI (1992) 127–131.
[31] M.I. Angelova, D.S. Dimitrov, Liposome electroformation, Faraday Discussions of the Chemical Society 81 (1986) 303–311.
[32] H.V. Ly, M.L. Longo, The influence of short-chain alcohols on interfacial tension, mechanical properties, area/molecule, and permeability of fluid lipid bilayers, Biophysical Journal 87 (2) (2004) 1013–1033.
[33] D.J. Lichlyter, M.A. Haidekker, Immobilization techniques for molecular rotors–towards a solid-state viscosity sensor platform, Sensors and Actuators B: Chemical 139 (2) (2009) 648–656.
[34] S. Kyu Han, J.-S. Kim, Y.-S. Lee, M. Kim, Effect of drug substances on the microviscosity of lipid bilayer of liposomal membrane, Archives of Pharmacal Research 13 (1990) 192–197.
[35] J.A. Levitt, M.K. Kuimova, G. Yahioglu, P.-H. Chung, K. Suhling, D. Phillips, Membrane-bound molecular rotors measure viscosity in live cells via fluorescence lifetime imagingâ, The Journal of Physical Chemistry C 113 (27) (2009) 11634–11642.
[36] M.K. Kuimova, G. Yahioglu, J.A. Levitt, K. Suhling, Molecular rotor measures viscosity of live cells via fluorescence lifetime imaging, Journal of the American Chemical Society 130 (21) (2008) 6672–6673.
[37] A. Hawe, V. Filipe, W. Jiskoot, Fluorescent molecular rotors as dyes to characterize polysorbate-containing IgG formulations, Pharm Res 27 (2) (2010) 314–326.
[38] M. Chachisvilis, Y.L. Zhang, J.A. Frangos, G protein-coupled receptors sense fluid shear stress in endothelial cells, Proceedings of the National Academy of Sciences of the United States of America 103 (42) (2006) 15463–15468.
[39] R.O. Loutfy, B.A. Arnold, Effect of viscosity and temperature on torsional relaxation of molecular rotors, The Journal of Physical Chemistry 86 (21) (1982) 4205–4211.
[40] C.E. Kung, J.K. Reed, Microviscosity measurements of phospholipid bilayers using fluorescent dyes that undergo torsional relaxation, Biochemistry 25 (20) (1986) 6114–6121.